9

Mathematical Modeling of Single Peak Dynamic Recrystallization Flow Stress Curves in Metallic Alloys

R. Ebrahimi and E. Shafiei
Department of Materials Science and Engineering, School of Engineering, Shiraz University, Shiraz, Iran

1. Introduction

Deformation of metals and alloys at temperatures above 0.5 T_m is a complex process in which mechanical working interacts with various metallurgical processes such as dynamic restoration including recovery and recrystallization, and phase transformation for polymorphous materials. The understanding of these processes, however, enables the behavior of the metals and alloys. Recent developments have been described in several review papers. These reviews were in agreement that metals and alloys having relatively low values of stacking fault energy (SFE) could recrystallize dynamically, whereas those of high SFE including bcc metals and alloys which behave in a manner similar to fcc metals of high SFE recovered dynamically only during high temperature deformation. So that, according to microstructural evolutions, material response can principally be divided into two categories in hot deformation: dynamic recovery (DRV) type and dynamic recrystallization (DRX) type.

The process of recrystallization of plastically deformed metals and alloys is of central importance in the processing of metallic alloys for two main reasons. The first is to soften and restore the ductility of material hardened by low temperature deformation that occurring below about 50% of the absolute melting temperature which leads to lower forces. The second is to control the microstructure and mechanical properties of the final product.

The analysis of metal forming process such as hot rolling, forging and extrusion has been dependent on various parameters including constitutive relation which contributes to stress-strain curves at high temperatures, shape of workpiece and product, shapes of tools, friction, temperature, forming speed, etc. In such parameters, the constitutive equation is one of the most important factors which have an effect on solution accuracy.

A number of research groups have attempted to develop constitutive equations of materials and suggested their own formulations by putting the experimentally measured data into one single equation. Misaka and Yoshimoto proposed a model which gives the flow stress of carbon steels as a function of the strain, strain rate, temperature and carbon content. Shida's model takes account of the flow stress behavior of the steels in austenite, ferrite and in the

two-phase regions. Voce suggested an approximate equation of stress–stain curve considering the dynamic recrystallization. Finally, Ebrahimi et al. obtained a mathematical model according to the phenomenological representation of the shape of the stress-strain curves that consists an additional constant. Due to the importance of flow stress estimation of metals and alloys at high temperatures, the required forces for the deformation processes, dimensional accuracy of final products and simulation of processes; it is necessary to provide a model in order to eliminate the limitations of previous models to some extent. The contexts of this section could generally be classified into two main parts, at the beginning, some previous mathematical models and basic concepts in relation with dominate processes during hot deformation of metals and alloys, such as dynamic recovery (DRV) and dynamic recrystallization (DRX) will be reviewed and finally, by concluding from existing mathematical models related to prediction of single peak flow stress curves, a new model will be introducd. With regards to the importance of macroscopic data from mechanical tests as compared to microscopic ones from metallurgical investigation, due to its less time and cost consuming nature, mathematical and macroscopic aspects of DRX process are considered in this model.

2. Basic concepts

2.1 Dynamic recovery (DRV)

The basic mechanisms of dynamic recovery are dislocation climb, cross-slip and glide, which result in the formation of low angle boundaries as also occurs during static recovery. However, the applied stress provides an additional driving pressure for the movement of low angle boundaries and those of opposite sign will be driven in opposite directions, and this stress-assisted migration of dislocation boundaries may contribute significantly to the overall strain.

Such migration results in some annihilation of dislocations in opposing boundaries and Y-junction boundary interactions and these enable the subgrains to remain approximately equiaxed during the deformation. In-situ SEM deformation experiments have shown that some reorientation of subgrains may also occur during hot deformation. The subgrains can therefore be considered to be transient microstructural features.

The processes of work hardening and recovery lead to the continual formation and dissolution of low angle boundaries and to a constant density of unbound or ‘free’ dislocations within the subgrains. After a strain of typically 0.5 to 1, the subgrain structure often appears to achieve a steady state. The microstructural changes occurring during dynamic recovery are summarized schematically in figure 1.

2.2 Dynamic recrystallization (DRX)

In metals which recovery processes are slow, such as those with a low or medium stacking fault energy (copper, nickel and austenitic iron), dynamic recrystallization may take place when a critical deformation condition is reached. A simplified description of the phenomenon of dynamic recrystallization is as follows. As shown in figures 2, new grains originate at the old grain boundaries, however, as the material continues to deform, the dislocation density of the new grains increases, thus reducing the driving force for further growth, and the recrystallizing grains eventually cease to grow. An additional factor which may limit the growth of the new grains is the nucleation of further grains at the migrating boundaries.

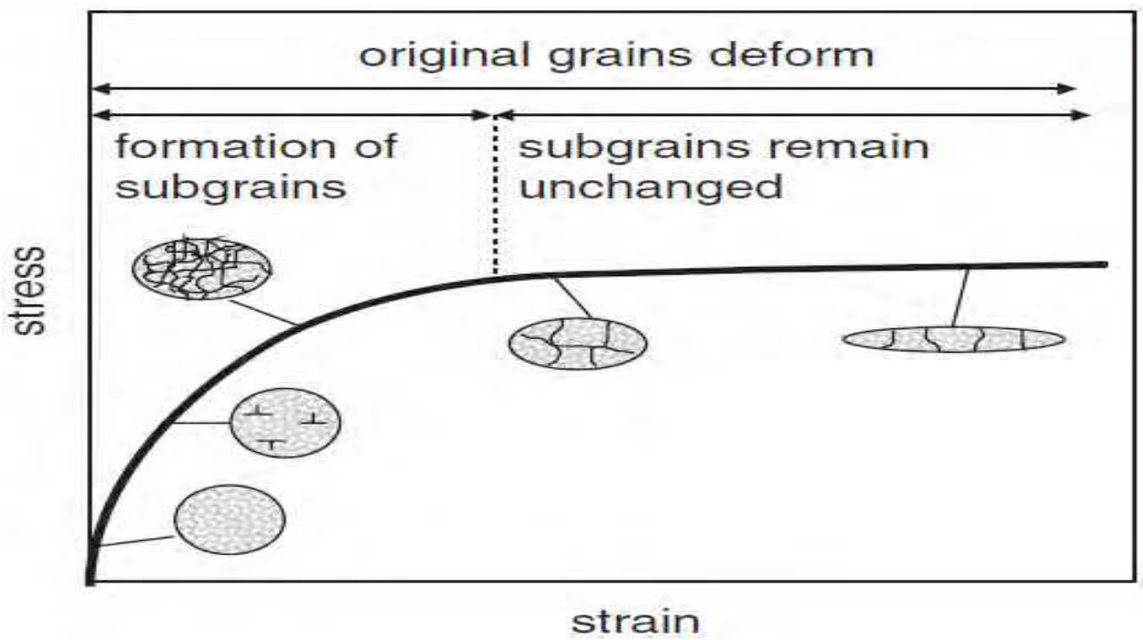

Fig. 1. Summary of the microstructural changes which occur during dynamic recovery.

This type of dynamic recrystallization, which has clear nucleation and growth stages, can be classified as a discontinuous process. There are other mechanisms which produce high angle grain boundaries during high temperature deformation and which may be considered to be types of dynamic recrystallization such as continuous dynamic recrystallixation (CDRX).

The general characteristics of dynamic recrystallization are as follows (Humphreys et al., Elsevier):

- As shown in figure 3, the stress-strain curve for a material which undergoes dynamic recrystallization generally exhibits a broad peak that is different to the plateau, characteristic of a material which undergoes only dynamic recovery (fig.1). Under conditions of low Zener–Hollomon parameter, multiple peaks may be exhibited at low strains, as seen in figure 3.
- A critical deformation is necessary in order to initiate dynamic recrystallization.
- The critical deformation decreases steadily with decreasing stress or Zener–Hollomon parameter (description in section 3.2), although at very low strain rates (creep) the critical strain may increase again.
- The size of dynamically recrystallized grains increases monotonically with decreasing stress. Grain growth does not occur and the grain size remains constant during the deformation.
- The flow stress and grain size are almost independent of the initial grain size, although the kinetics of dynamic recrystallization are accelerated in specimens with smaller initial grain sizes.
- Dynamic recrystallization is usually initiated at pre-existing grain boundaries although for very low strain rates and large initial grain sizes, intragranular nucleation becomes more important.

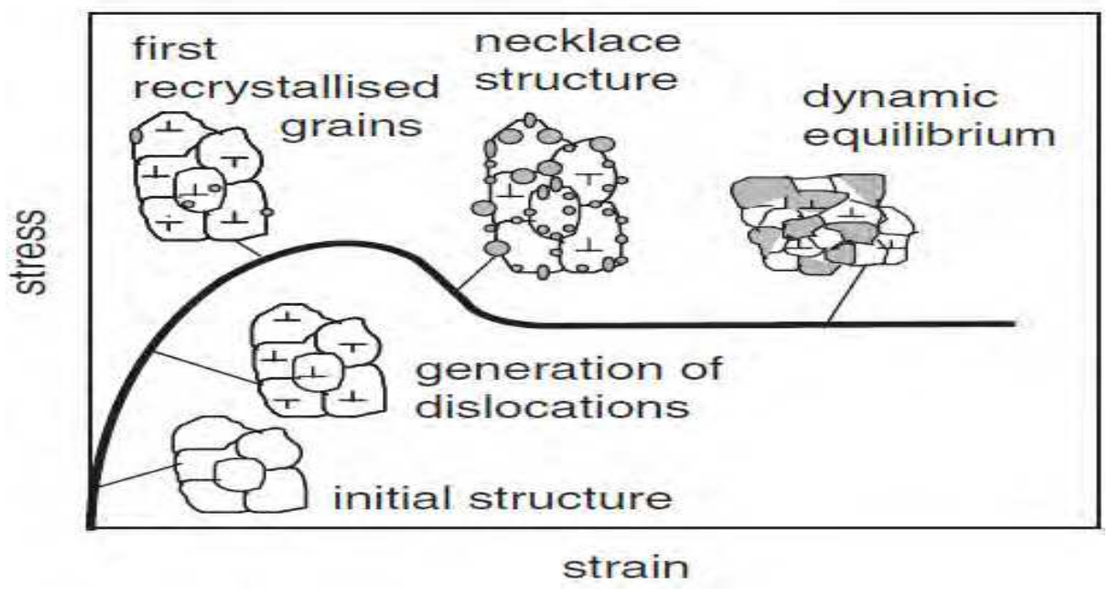

Fig. 2. Evolution of microstructure during hot deformation of a material showing DRX.

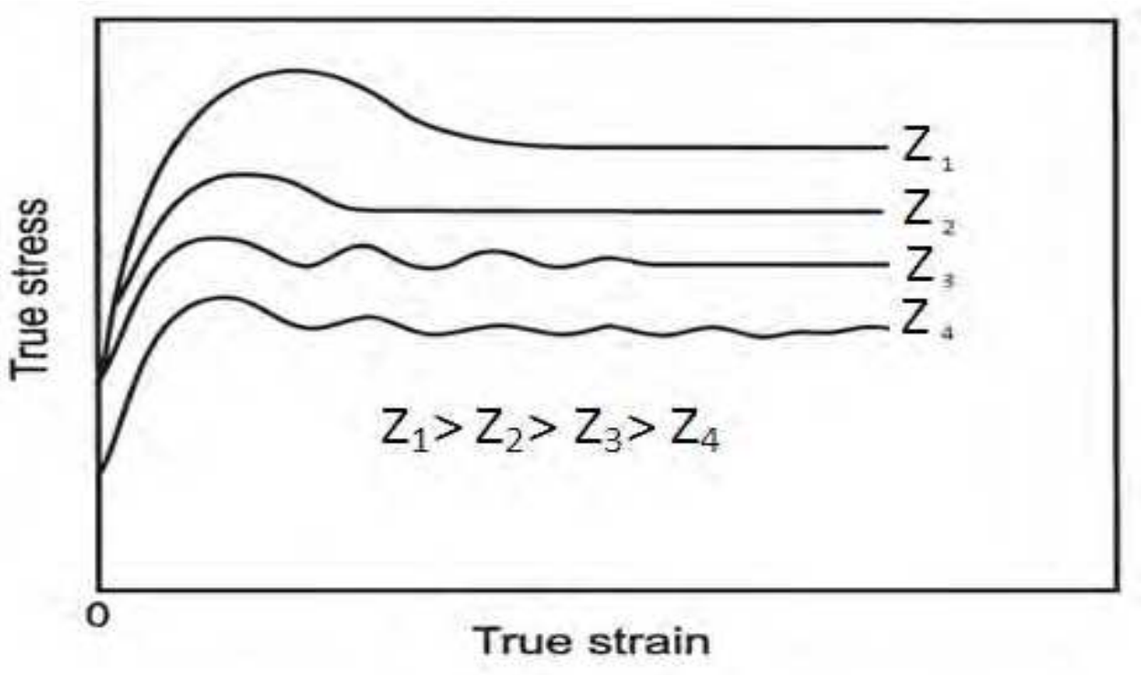

Fig. 3. The effect of Zener Hollomon parameter on the stress- strain curve.

2.3 Test methods

There are many different types of test methods, such as hot torsion, compression, tension, cam plastometer and drop hammer for developing the constitutive equation of the materials behavior. Among them, hot torsion and compression tests have widely been used. Hot torsion test has been used by many researchers to formulate constitutive equation of materials subject to a large strain because it has a forte in simulating the multi-pass deformation, in comparison with axisymmetric compression test. In the case of compression test, high friction at the interface of material and stroke head results in barreling during test. Thus, the compression test has a limitation in generating flow stress curve when the material undergoes large strain. Also Kim et al. have shown that the flow stress obtained from compression test is higher than that from torsion test, although the general shapes of the measured curves are similar. The differences between the stresses were approximately in the range of 10–20%.

These differences might be attributed to the following reasons: compression test has the glowing frictional forces at the ram-specimen interface as the test progress, while, there is no frictional effect in torsion test. In compression test, it is difficult to achieve constant strain rate and isothermal condition during test, whereas to control them in torsion test is accurate.

2.4 Flow curves

For metals with high stacking fault energy which experience DRV, the flow stress curves increase with strain in the initial deformation and reach constant in consequence of attaining the balance between work hardening and DRV (saturation stress, σ_s). For metals with DRX, initially the flow stress increases with strain which is being dominated by work hardening, and as DRX takes place upon critical strain (ε_c), the flow stress begins to decrease after reaching certain peak value. When the equilibrium is reached between softening due to DRX and work hardening, the curves drop to a steady state region (σ_{ss}). As shown in figure 3, the stress strain curves of a dynamically recrystallizing material may be characterized by a single peak or by several oscillations. Luton and Sellars have explained this in terms of the kinetics of dynamic recrystallization. At low stresses, the material recrystallizes completely before a second cycle of recrystallization begins, and this process is then repeated. The flow stress, which depends on the dislocation density, therefore oscillates with strain. At high stresses, subsequent cycles of recrystallization begin before the previous ones are finished, the material is therefore always in a partly recrystallized state after the first peak, and the stress strain curve is smoothed out, resulting in a single broad peak. Fig. 4 shows a schematic representing of dynamic recovery and a single peak dynamic recrystallization.

2.5 Strain hardening rate versus stress

The change in the slope ($\Theta=d\sigma/d\varepsilon$) of the stress-strain curve with stress can be a good indication of the microstructural changes taking place in material. All of the Θ-σ curves for a particular alloy originate from a common intercept Θ_0 at $\sigma=0$. The Θ-σ curves have three segments, two of them are linear. The first linear segment decreases with stress for initial strain to the point where subgrains begin to form with a lower rate of increase in DRV. The curve gradually changes to the lower slope of the second linear segment up to the point

where the critical stress σ_c is attained for initiating the dynamic recrystallization. The curve then drops off rather sharply to $\Theta=0$ at peak stress. Extrapolation of the second linear segment of the Θ-σ curve intercepts the σ axis at the saturation stress. This would be the shape of the Θ-σ curve if dynamic recrystallization were absent with only dynamic recovery as the restorative mechanism operation, Fig.5.

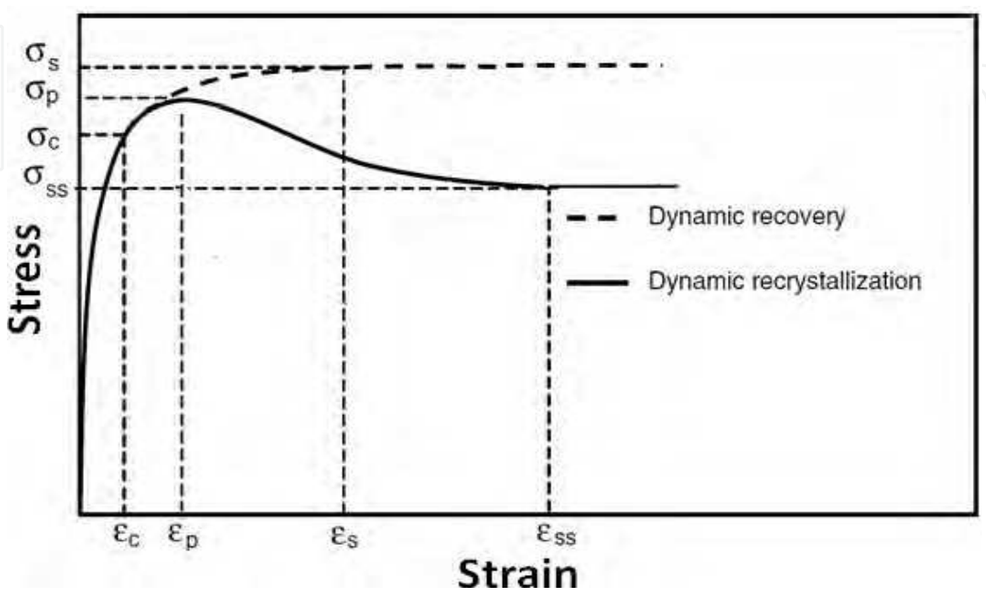

Fig. 4. Schematic representing of DRV and DRX.

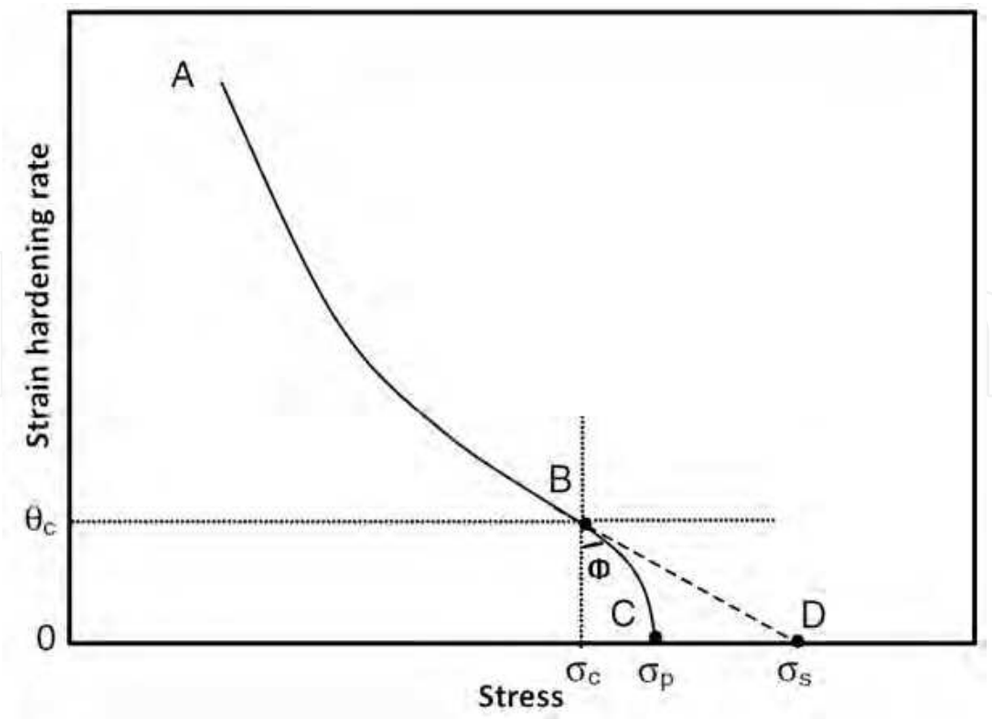

Fig. 5. Changes in the slope of the stress-strain curve with stress.

3. A review on presented models

Considerable researches have been carried out to model flow stress curves at high temperatures based on both empirical and mathematical models. Empirical models which are based on trial and error mainly obtained by repeating the mechanical tests at different conditions, and among these models, Shida and Misaka models could be mentioned. The most important limitation of these types of models is that they are valid for specific conditions and cannot be generalized, whereas in mathematical models, in order to estimate the flow curve, the material response are modeled first and then the empirical data is used to verify the prediction. Among these models, Cingara, Kim et.al and Ebrahimi et.al could be mentioned. According to the presented models, some limitations could be considered in this category, too. For instance, the presented model by McQueen and Cingara for DRX is only valid up to the peak stress (σ_p) and does not consider the softening behavior due to DRX, although a complement model has been developed to predict the softening behavior due to DRX.

Mathematical modeling of flow stress curves can be divided into three main topics as follows:

- Mathematical models which characterize the initiation of DRX.
- Mathematical models which predict characteristic points of flow stress curves.
- Mathematical models which predict flow stress curves.

It is important to mention that, due to less time and cost consuming nature of mathematical and macroscopic models, only this aspect of DRX process is considered in this chapter.

3.1 Initiation of dynamic recrystallization

The critical strain for initiation of DRX could be determined by metallography. However, this technique requires extensive sampling before and after the critical strain. Furthermore, phase changes during cooling from hot working temperature alter the deformed structure, which in turn render difficulties for metallographic analysis. Also this technique requires a large number of specimens deformed to different strains. On the other hand, the critical strain thus obtained is not precise.

Several attempts have been made to predict the initiation of DRX. For example, Ryan and McQueen observed that the presence of a stress peak at a constant strain rate flow curve leads to an inflection in plots of strain hardening rate, θ, versus stress, σ. Moreover, the points of inflection in θ-σ plots where the experimental curves separate from the extrapolated lower linear segments give critical conditions for initiation of DRX. Later, Poliak and Jonas have shown that this inflection point corresponds to the appearance of an additional thermodynamic degree of freedom in the system due to the initiation of DRX.

3.1.1 Determination of critical stress

The simple method of Najafizadeh and Jonas was used for determination of the critical stress for initiation of DRX. The inflection point is detected by fitting a third order polynomial to the θ-σ curves up to the peak point as follows:

$$\theta = A\sigma^3 + B\sigma^2 + C\sigma + D \tag{1}$$

where *A*, *B*, *C*, and *D* are constants for a given set of deformation conditions. The second derivative of this equation with respect to σ can be expressed as:

$$\frac{d^2\theta}{d\sigma^2} = 6A\sigma + 2B \tag{2}$$

At critical stress for initiation of DRX, the second derivative becomes zero. Therefore,

$$6A\sigma_c + 2B = 0 \Rightarrow \sigma_c = \frac{-B}{3A} \tag{3}$$

An example of θ-σ curves and its corresponding third order polynomial are shown in Fig. 6. Therefore, this method is used to determine the value of critical stress at different deformation conditions. Using the flow curves, the values of critical strain are determined (Najafizadeh et al. 2006).

According to Fig. 7, the normalized critical stress and strain for 17-4 PH stainless steel could be presented as:

$$\frac{\sigma_c}{\sigma_p} = 0.89 \tag{4}$$

$$\frac{\varepsilon_c}{\varepsilon_p} = 0.467 \tag{5}$$

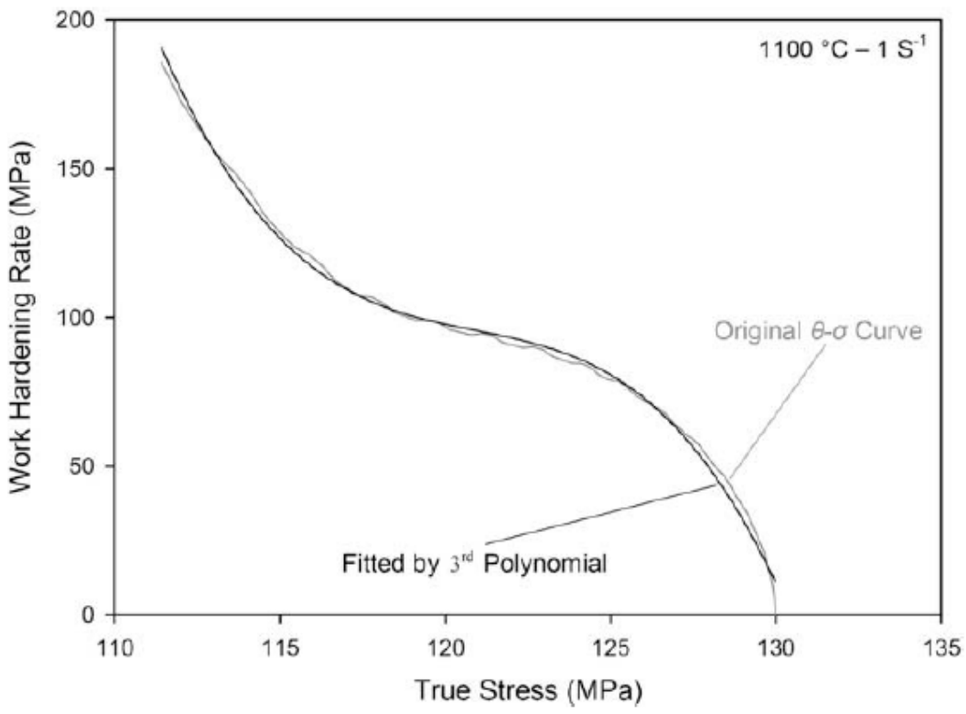

Fig. 6. The θ-σ curve of 17-4 PH Stainless steel and its corresponding third order polynomial.

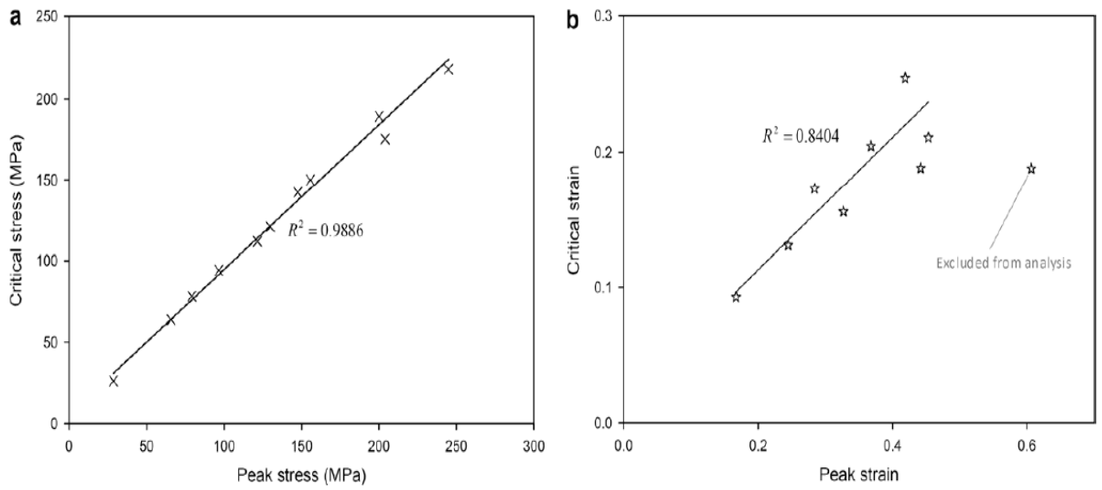

Fig. 7. Critical stress and strain versus (a) peak stress and (b) peak strain.

3.1.2 Determination of critical strain, (Poliak and Jonas)

Poliak and Jonas have shown that the inflection in plots of lnΘ-ε and lnΘ-σ curves can also be used for determination of initiation of DRX. The procedure of Section 3.1.1 is used to determine the values of critical strain at different deformation conditions (Mirzadeh et al., 2010).

According to figure 8, the normalized critical strain could be presented for 17-4 PH stainless steel:

$$\frac{\varepsilon_c}{\varepsilon_p} = 0.47 \tag{6}$$

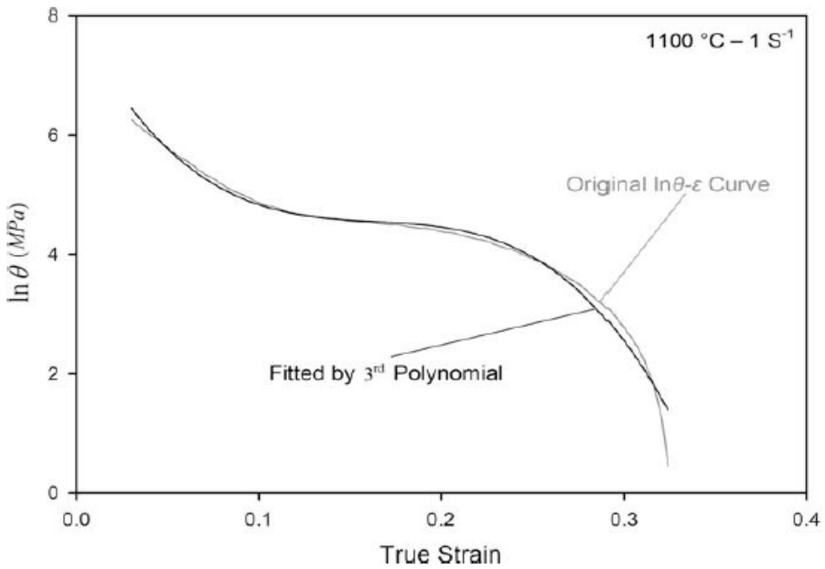

Fig. 8. The lnΘ-ε curve for 17-4 PH stainless steel and its corresponding third order polynomial.

3.1.3 Determination of critical strain (Ebrahimi and Solhjoo)

The flow stress up to the peak stress was modeled using the Cingara and McQueen equation as shown below:

$$\sigma = \sigma_p[(\varepsilon / \varepsilon_p)\exp(1-\varepsilon / \varepsilon_p)]^C \tag{7}$$

Where constant C is an additional parameter to make the results acceptable and is obtained from logarithmic form of Eq.7. The derivative of the true stress with respect to true strain yields the work hardening rate, Θ. Therefore, the Θ formula using Eq.7 may be expressed as:

$$\theta = C\sigma(1/\varepsilon - 1/\varepsilon_p) \tag{8}$$

In order to determine the critical strain, the second derivative of Θ with respect to σ must be zero. By solving this equation, the critical strain as a function of peak strain will obtain as follows:

$$\frac{\varepsilon_c}{\varepsilon_p} = \frac{\sqrt{1-C} - (1-C)}{C} \tag{9}$$

The results showed a good agreement with the experimentally measured ones for Nb-microallyed steel (Ebrahimi et al., 2007).

3.2 Kinetic equations (prediction of single points)

The influence of temperature and strain rate on peak stress was analyzed by the following equations which were originally developed for creep but have found applicability in the high strain rates in hot working:

$$A'\sigma_p^{n''} = \dot{\varepsilon}\exp\left(\frac{Q_{HW}}{RT}\right) = Z \tag{10}$$

$$A''\exp(\beta\sigma_p) = \dot{\varepsilon}\exp\left(\frac{Q_{HW}}{RT}\right) = Z \tag{11}$$

$$A'''\left[\sinh(\alpha\sigma_p\right]^n = \dot{\varepsilon}\exp\left(\frac{Q_{HW}}{RT}\right) = Z \tag{12}$$

where $A', A'', A''', n, n'', Q_{HW}, a, \beta$ and R are constants and Z is the Zener Hollomon. Q_{HW} is the activation energy related to hot working and R is the universal gas constant. A power law plot of log σ versus log Z gives linear segments only at low stress, indicating the limited applicability of Eq. (10). However in a plot of σ against log Z linearity is lost at low stress, showing that Eq. (11) is an inadequate fit for the entire range of stresses. Eq. (12) is a more general form of Eq. (10) and Eq. (11) reducing to Eq. (10) at lower stresses ($\alpha\sigma<0.8$) and Eq. (11) at higher stresses ($\alpha\sigma>1.2$). The validation of these equations to predict characteristic points of flow curves were approved by many authors (Cingara et al., 1992).

3.3 Experimental models

3.3.1 Misaka's model

Misaka and Yoshimoto have utilized the following double-power constitutive equation to determine flow stress associated with the processing of steels:

$$\sigma_{Misaka} = 9.8\exp\left(0126 - 1.75[C] + 0.594[C]^2\right) + \left(\frac{2851 + 2968[C] - 1120[C]^2}{T + 273}\right)\varepsilon^n \dot{\varepsilon}^m \quad (13)$$

Application range of this formula is as follows; carbon content: ≈1.2%, temperature: 750–1200 ^{o}C, reduction (natural strain): 50% and strain rate: 30–200 s^{-1}. Misaka's equation was updated by including effects of solution-strengthening and dynamic recrystallization.

The updated Misaka's constitutive equation is:

$$\sigma_{Misaka,Updated} = \left(f\sigma_{Misaka}\right)\left(1 - X_{DRX}\right) + k\sigma_{ss}X_{DRX} \quad (14)$$

$$f = 0.835 + 0.51[Nb] + 0.098[Mn] + 0.128[Cr]^{0.8} + 0.144[Mo]^{0.3} + 0.175[V] + 0.01[Ni] \quad (15)$$

(σ_{Misaka})updated indicates the flow stress of steels containing multiple alloying additions. σ_{ss} is steady state stress, K =1.14 is a parameter that converts flow stress to mean flow stress, and X_{DRX} is volume fraction of dynamic recrystallization. It might be useful for practical purpose but its mathematical base is weak. The factors for Mn, Nb, V and Ni are linear although the terms for Cr and Mo are nonlinear. Devadas et al. compared the predicted flow stress data for a low alloy steel with measured data from a cam-plastometer. They showed that Misaka's model overestimated the flow stress (Kim et al., 2003).

3.3.2 Shida's equation

Shida's equation is based on experimental data obtained from compression type of high strain rate testing machines. Shida then expressed the flow stress of steels, σ, as a function of the equivalent carbon content (C), the strain (ε), the strain rate ($\dot{\varepsilon}$) and temperature (T) as followings:

$$\sigma = \sigma_d(C,T)\, f_w(\varepsilon)\, f_r\left(\dot{\varepsilon}\right) \quad (16)$$

$$\sigma_d = 0.28\exp\left(\frac{5}{T} - \frac{0.01}{C + 0.05}\right) \quad (17)$$

$$T[k] = \frac{T\left[^oC\right] + 273}{1000} \quad (18)$$

$$f_w(\varepsilon) = 1.3\left(\frac{\varepsilon}{0.2}\right)^n - 0.3\left(\frac{\varepsilon}{0.2}\right) \quad (19)$$

$$n = 0.41 - 0.07C \tag{20}$$

$$f_r\left(\dot{\varepsilon}\right) = \left(\frac{\dot{\varepsilon}}{10}\right)^m \tag{21}$$

$$m = \left(-0.019C + 0.126\right)T + \left(0.076C - 0.05\right) \tag{22}$$

where $f_w(strain)$ and f_r(strain rate) are functions dependent upon strain and strain rate, respectively. The formulation of Eq. (16) is based on assumption that flow stress increases with the strain rate and strain increased. The range of validity of the formula is quite broad. This formula is applicable in the range of carbon content: 0.07–1.2%, temperature: 700–1200°C, strain: ≈ 0.7 and strain rate: ≈100 s^{-1}.

3.3.3 Modified Voce's equation

In contrast to Misaka's and Shida's equations, Voce's equation can describe the flow stress over the wide range of strains and strain rates. The equation can express the dynamic softening portion of the flow stress curve by using Avrami equation:

$$\sigma_{WH+DRV} = \sigma_p\left[1 - \exp\left(-c\varepsilon\right)\right]^m \tag{23}$$

The coefficient, *C*, and work hardening exponent, *m*, are dependent on the deformation conditions. The parameters, *C* and *m* are normally taken as being a constant, however, it is a function of the deformation conditions (strain rate, temperature). Thus, the *C* and *m* are considered to be a function of dimensionless parameter, *Z*/*A*.

Also Kim et al. developed an equation by modifying Voce's constitutive equations accounting for the dynamic recrystallization as well as the dynamic softening. During thermomechnical processing, the important metallurgical phenomena are work hardening (WH), dynamic recovery (DRV) and dynamic recrystallization (DRX). Thus, the flow stress curve can be bisected with the WH + DRV region and the DRX region. For the evaluation of the WH and DRV region, Eq. 23 was used. Also For the region of DRX, the drop of flow stress was expressed as the following equation:

$$\sigma_{Drop} = \left(\sigma_p - \sigma_{ss}\right)\left[\frac{X_{DRX} - X_{\varepsilon_p}}{1 - X_{\varepsilon_p}}\right] \quad \text{for } \varepsilon > \varepsilon_p \tag{24}$$

Therefore, the flow stress can be expressed in subtraction form as follows:

$$\sigma = \sigma_{WH+DRV} - \sigma_{Drop} \tag{25}$$

where σ_{ss} is the steady state stress achieved at larger strains and $X_{\varepsilon p}$ the volume fraction of DRX at peak strain. X_{DRX} is the volume fraction of DRX at any strain.

Fig. 9 shows the measured and predicted flow stress curves in large strain range of AISI 4140 steel when the three different types of constitutive equations are used for prediction. The flow stress curves calculated by using Misaka's equation agree with the measured ones with some extent of error in comparison to the flow stress curve obtained from Shida's equation. Although, the stress–strain curves predicted by using the modified Voce's equation are in a good agreement with experimentally measured ones, it seems Misaka's equation does not reflect recrystallization behavior properly (Kim et al., 2003).

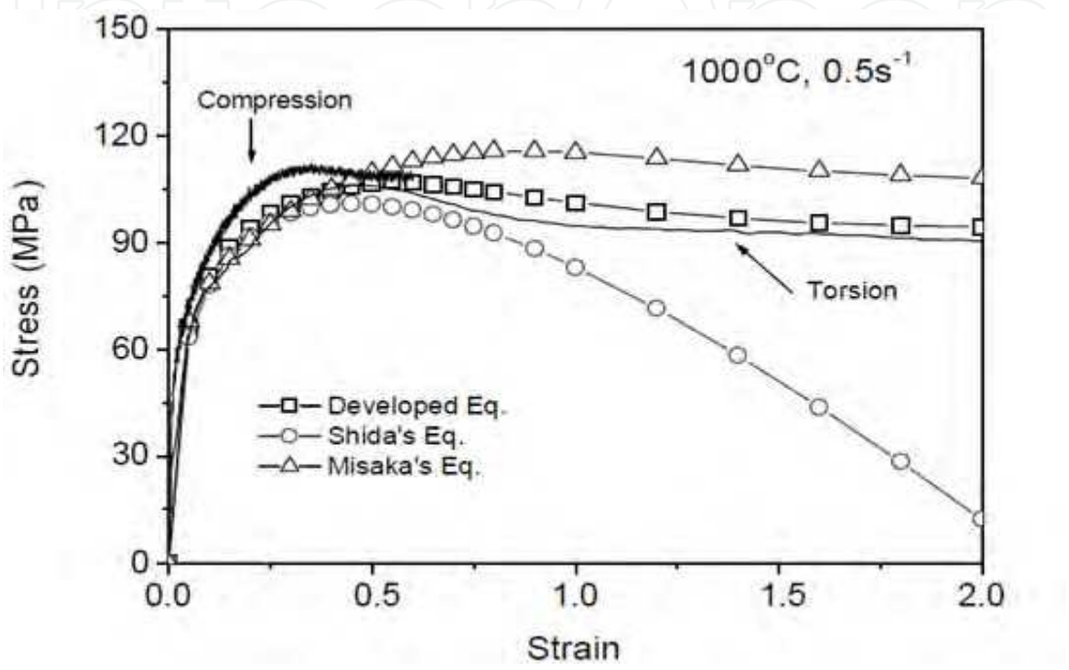

Fig. 9. Comparison of measured and predicted constitutive relations for AISI 4140 steel.

3.4 Mathematical models

3.4.1 Solhjoo's model

Solhjoo was considered linear estimation of θ-σ curve up to the peak stress as follows:

$$\frac{\partial \sigma}{\partial \varepsilon} = S_4 + A_1 \tag{26}$$

where S_4 is the slope of the line and A_1 is a constant. Due to the first assumption which considers a linear segment up to the peak, this model would not be able to show the critical strain. Using the maximum point of the θ-σ curve ($\sigma=\sigma_p,\theta=0$), value of constant A_1 is obtained to be $-S_4\sigma_p$. Solution of the differential Eq. (26) with respect to ε, using boundary condition $\sigma=\sigma_p$ at $\varepsilon=\varepsilon_p$is:

$$\sigma = \sigma_p \left[1 - \left(\frac{\left(\varepsilon_p - \varepsilon\right)}{\varepsilon_p} \right) \exp\left(S_4 \varepsilon\right) \right] \tag{27}$$

where σ_p is the peak stress and ε_p is the peak strain.

Determination of S_4 can be simply done using a linear plot of $\ln\left(\frac{\varepsilon_p}{\sigma_p}\frac{\sigma_p-\sigma}{\varepsilon_p-\varepsilon}\right)$ vs. ε; S_4 would be the slope of the line. As S_4 is very sensitive to strain rate, it is better to plot $\ln\left(\frac{\varepsilon_p}{\sigma_p}\frac{\sigma_p-\sigma}{\varepsilon_p-\varepsilon}\right)$ vs. ε for each sets of strain rates, and then the average value of the slopes determines S_4. Assuming S_4 as a constant shows a rough estimation of stress– strain curve. Since S_4 is more sensitive to strain rate than temperature, this parameter can be considered as a power law in form of:

$$S_4 = -C\dot{\varepsilon}^{E} \tag{28}$$

where E is strain rate and C and ε are constants. Using a plot of ln(-S4) vs. $\dot{\varepsilon}$, constants C and E can be determined. It should be considered that another limit of this model is its disability of prediction of flow stress at very low strains (less than 0.05) that the work hardening rate has very high values (Solhjoo, 2009).

3.4.2 Avrami's analysis

The DRX may be considered as a solid-state transformation and its kinetics can be modeled by the Johnson–Mehl–Avrami–Kolmogorov (JMAK) equation as follows:

$$X_{DRX} = 1 - \exp\left(-kt^n\right) \tag{29}$$

where X_{DRX} *and* t are the recrystallized volume fraction and DRX time, respectively. The effect of dynamic recovery (DRV) on flow softening was not considered. Therefore, this model is preliminary intended for materials with relatively low stacking fault energy. Moreover, for modeling the flow curves after the peak point of stress–strain curve, the initiation of DRX was intentionally considered at peak point. This assumption simplifies the Avrami analysis with acceptable level of accuracy. Therefore, Eq. (30) gives the magnitude of flow stress at each fractional softening:

$$\sigma = \sigma_p - \left(\sigma_p - \sigma_{ss}\right)X_{DRX} \tag{30}$$

3.4.3 Ebrahimi's model

This model is based on a phenomenological representation of the shape of the flow stress curves and the traditional theories for constitutive equations which incorporate the power law. Ebrahimi et al. considered the variations of the slope of flow stress curves as follows:

$$\frac{d\sigma}{d\varepsilon} = C_1\left(\sigma - \sigma_{ss}\right)\left(1 - \frac{\varepsilon}{\varepsilon_p}\right) \tag{31}$$

Where ε_p is the strain at the peak stress and σ_{ss} is the steady state stress. The term $(1-\varepsilon/\varepsilon_p)$ estimates variation of the stress- strain curve for $\sigma>\sigma_{ss}$. Solution of the differential Eq.(31) with respect to ε using boundary condition $\sigma=\sigma_p$ at $\varepsilon=\varepsilon_p$ results in:

$$\sigma = \sigma_{ss} + \left(\sigma_p - \sigma_{ss}\right)\exp\left[C_1\left(\varepsilon - \frac{\varepsilon_p}{2} - \frac{\varepsilon^2}{2\varepsilon_p}\right)\right] \tag{32}$$

If $\varepsilon=\varepsilon_k$ and $\varepsilon_k=k\varepsilon_p$ where $k<1$ and $\sigma_k>\sigma_{ss}$, then coefficient C_1 can be estimated from Eq. (33) as:

$$C_1 = \frac{2}{\left(k^2 - 2k + 1\right)\varepsilon_p}\ln\left(\frac{\sigma_p - \sigma_{ss}}{\sigma_k - \sigma_{ss}}\right) \tag{33}$$

Where σ_k is the stress calculated from Cingara equation. The equation represented by this model required the values of stress and strain at the peak and stress at the steady state zone. These parameters can be calculated by kinetic equations (Ebrahimi et al., 2006).

Fig. 10 shows the calculated flow curves by Cingara, Avrami and Ebrahimi et al. equations. At low Z, the predictions of Ebrahimi et al. equation are relatively accurate (Fig. 10a), but at high Z, this equation overestimates the flow softening of DRX (Fig. 10c). In other words, this equation seems to be suitable for ideal DRX behavior. The Ebrahimi et al. equation is based on a phenomenological representation of the shape of the stress–strain curves and the traditional theories for constitutive equations which incorporate the power law. Conversely, the Avrami equation is amenable to all deformation conditions as shown in Fig. 10. In fact, this equation is an adaptive one with two adjustable constants. As a result, it could be better fitted to hot flow curves. Therefore, the Avrami equation can be used for prediction of flow curves as shown in Fig. 10 (Mirzadeh et al., 2010).

3.4.4 Shafiei and Ebrahimi's constitutive equation

Using the extrapolation of DRV flow stress curves and kinetic equation for DRX, Shafiei and Ebrahimi proposed the following equation for modeling single peak DRX flow curves for $\varepsilon_c \le \varepsilon < \varepsilon_{ss}$

$$\sigma = \sigma_s - \left(\sigma_s - \sigma_c\right)\exp(C'\left(\varepsilon_c - \varepsilon\right)) - \left(\sigma_s - \sigma_{ss}\right)X_{DRX} \tag{34}$$

Where C′ is a constant with metallurgical sense. According to the geometrical relations shown in Fig.5, the value of C′ can be formulized as Eq.s (35) and (36) . σ_c, σ_p, σ_{ss}, σ_s , ε_c , X_{DRX} are critical stress, peak stress, steady state stress, saturation stress , critical strain and volume fraction of DRX, respectively.

$$\tan\varphi = \frac{1}{C'} \tag{35}$$

$$\varphi = \frac{\pi}{2} + Arctg\left(\frac{\sigma_p\varepsilon_p}{\varepsilon_c\left(\varepsilon_c - \varepsilon_p\right)}\right) \tag{36}$$

As shown in Fig.11, the stress-strain curves predicted by using presented model are in a good agreement with experimentally measured ones for Ti-IF steel. In order to evaluate the accuracy of the model, the mean error was calculated. The mean error of flow stress is calculated at strains of 0.19-2 for every measurement under all deformation conditions. For all stress-strain curves, the mean errors are between -2.9% and 2.5%. The results indicate that the proposed model give a good estimate of the flow stress curves. Therefore, it can be deduced that the approach to obtain a constitutive equation applicable to large strain ranges was fruitful and this presented model might have a potential to be used where more precise calculation of stress decrement due to dynamic recrystallization is important. Moreover, this analysis has been done for the stress-strain curves under hot working condition for Ti-IF steel, but it is not dependent on the type of material and can be extended for any condition that a single peak dynamic recrystallization occurs.

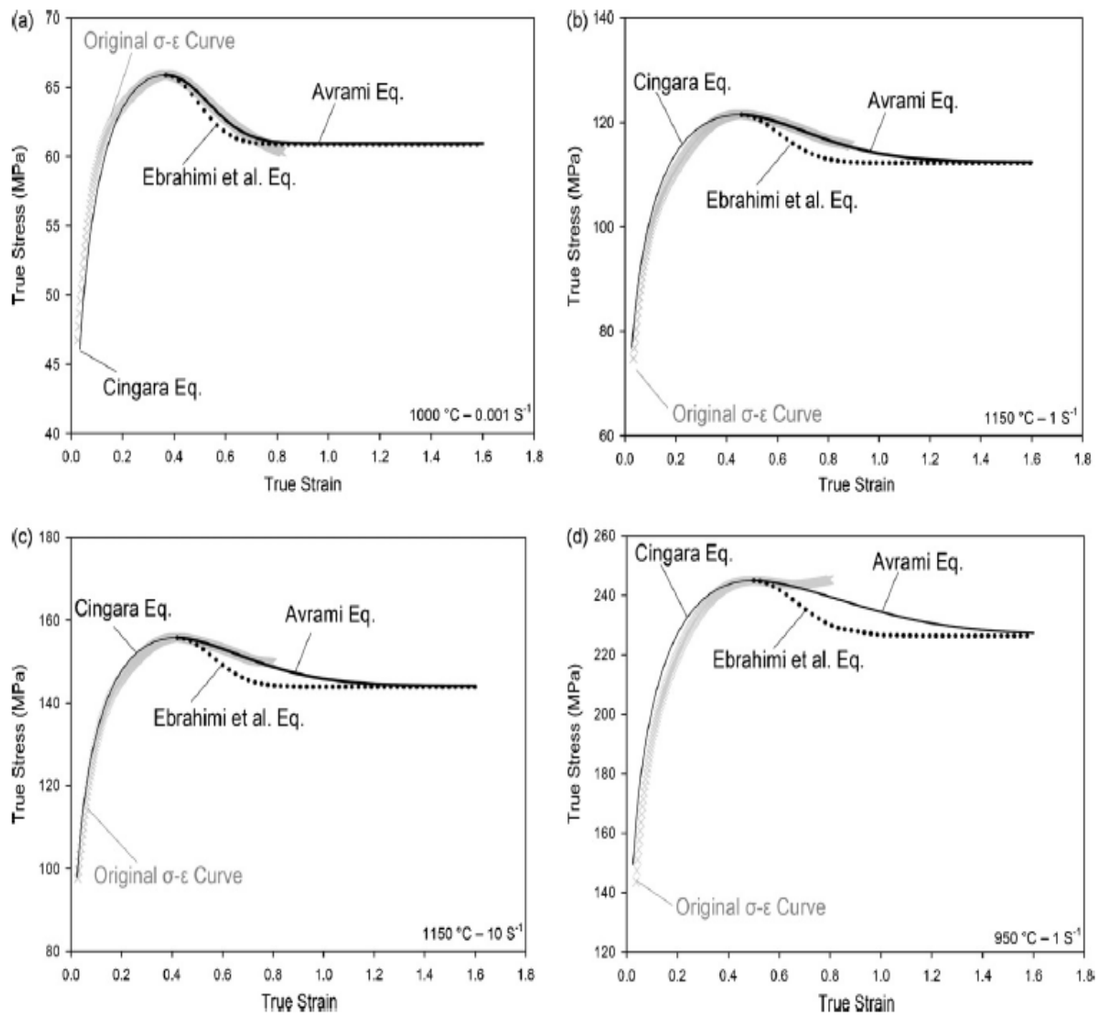

Fig. 10. Comparison between calculated and measured flow stress curves of 17-4 PH stainless steel.

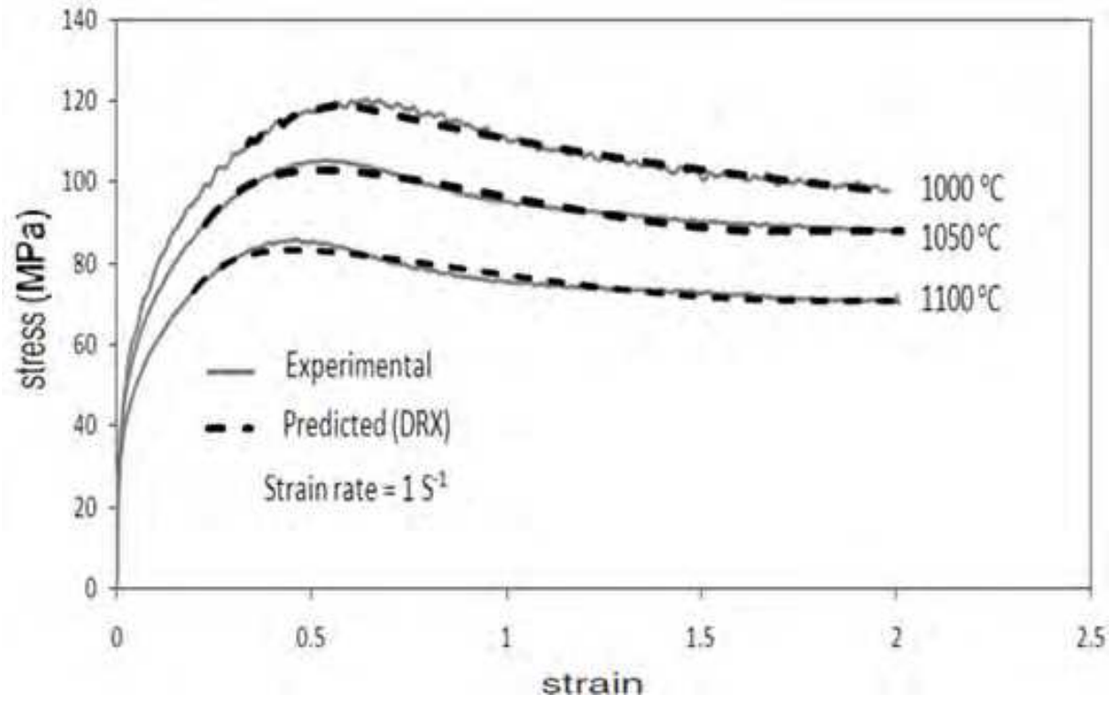

Fig. 11. Comparison of measured and predicted stress-strain curves of Ti-IF steel.

4. Summary

In this chapter, a review on recent model of single peak flow stress curves was presented. At first, the basic concepts on hot deformation and dynamic restoration, including affecting factors on dominated processes such as DRX and DRV and related microstructure evolutions were discussed. Then, an introduction on experimental models which are more capable in the field of industrials investigations such as Misaka, Shida and Voce constitutive equations followed by the details of mathematical models such as MC Queen, Ebrahimi, Solhjoo, Avrami and Shafiei- Ebrahimi constitutive equations were presented. In this case, the accuracy of these models as well as some limitations was evaluated in order to obtain the optimum working conditions.

5. References

Cingara, A. & McQueen, H. J. (1992). New method for determining sinh constitutive constants for high temperature deformation of 300 austenitic steel. Mater. Proc. And Tech, 36, 17-30.

Ebrahimi, R. & Solhjoo, S. (2007). Characteristic points of stress-strain curve at high temperature. ISSI, 2, 24-27.

Ebrahimi, R., Zahiri, S.H. & Najafizadeh, A. (2006). Mathematical modeling of the stress-strain curves of TI-IF steel at high temperature. Mater. Proc. And Tech., 171, 301-305.

Ebrahimi, R. (2003). Hot working of Ti-IF steel. Ph.D thesis. Isfahan University of Technology.

He, X. Yu, Zh. & Lai, X. (2008). A method to predict flow stress considering dynamic recrystallization during hot deformation. Comp. Mater. Sci., 44, 760-764.

Humphreys, F.J. & Hatherly, M. (2004). *Recrystallization and related annealing phenomena* (Second edition), (Elsevier, UK).

Imbert, C. A. C & McQueen, H. J. (2001). Peak strength, strain hardening and dynamic restoration of A2 and M2 tool steels in hot deformation. Mater. Sci. and Eng. A, 313, 88-103.

Imbert, C. A. C & McQueen, H. J. (2001). Dynamic recrystallization of A2 and M2 tool steels. Mater. Sci. and Eng. A, 313, 104-116.

Jonas, J. J., Quelennec, Jiang, L. & Martin, E. (2009). The avrami kinetics of dynamic recrystallization. Acta Mater. 137, 1748-2756.

Kim, S. I., Lee, Y. & Byon, S. M. (2003). Study on constitutive relation of AISI 4140 steel subject to large strain at elevated temperature. Mater. Proc. And Tech.,140, 84-89.

Liu, J., Cai, Zh. & Li, C. (2008). Modelling of flow stress characterizing dynamic recrystallization for magnesium alloys. Comp. Mater. Sci., 41,375-382.

Mirzadeh, H. & Najafizadeh, A. (2010). Extrapolation of flow curves at hot working conditions. Mater. Sci. and Eng. A, 527,1856-1860.

Mirzadeh, H. & Najafizadeh, A. (2010). Prediction of the critical conditions for initiation of dynamic recrystallization. Mater. And Des., 31, 1174-1179.

Najafizadeh, A. & Jonas, J. J. (2006). Predicting the critical stress for initiation of dynamic recrystallization. ISIJ Int., 46, 1679-1684.

Poliak, E. I. & Jonas, J. J. (2002). Initiation of dynamic recrystallization in constant strain rate hot deformation. ISIJ Int., 43, 684-691.

Shaban, M. & Eghbali, B. (2010). Determination of critical conditions for dynamic recrystallization of a microalloyed steel. Mater. Sci. and Eng. A, 527, 4320-4325.

Shafiei, E. & Ebrahimi, R. (2011). Mathematical modeling of single peak flow stress curves. Comp. Mater. Sci., submitted paper.

Solhjoo, S. (2009). Analysis of flow stress up to the peak at hot deformation. Mater. And Des.,30, 3036-3040.

Ueki, M., Horie, S. & Nakamura, T. (1987). Factors affecting dynamic recrystallization of metals and alloys. Mater. Sci. and Tech.,3, 329.

Verlinden, B., Driver, J., Samijdar, I. & Doherty, R. D. (2007). Thermomechanical processing of metallic materials. (Elsevier, Uk).

Zahiri, S. H., Davies, C. H. J. & Hodgson, P. D. (2005). A mechanical approach to quantify dynamic recrystallization in polycrystalline metals. Scripta Mater., 52, 299-304.

Zeng, Zh., Jonsson, S., Rovan, H. J. & Zhang, Y. (2009). Modelling the flow stress for single peak dynamic recrystallization. Mater. And Des.,30-1939-1943.

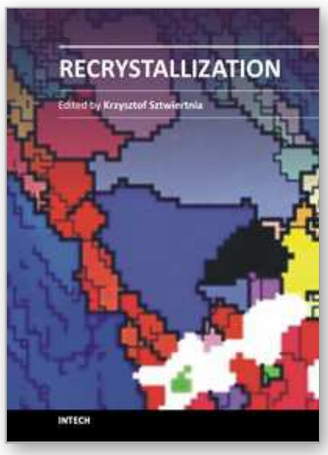

Recrystallization

Edited by Prof. Krzysztof Sztwiertnia

ISBN 978-953-51-0122-2
Hard cover, 464 pages
Publisher InTech
Published online 07, March, 2012
Published in print edition March, 2012

Recrystallization shows selected results obtained during the last few years by scientists who work on recrystallization-related issues. These scientists offer their knowledge from the perspective of a range of scientific disciplines, such as geology and metallurgy. The authors emphasize that the progress in this particular field of science is possible today thanks to the coordinated action of many research groups that work in materials science, chemistry, physics, geology, and other sciences. Thus, it is possible to perform a comprehensive analysis of the scientific problem. The analysis starts from the selection of appropriate techniques and methods of characterization. It is then combined with the development of new tools in diagnostics, and it ends with modeling of phenomena.

How to reference

In order to correctly reference this scholarly work, feel free to copy and paste the following:

R. Ebrahimi and E. Shafiei (2012). Mathematical Modeling of Single Peak Dynamic Recrystallization Flow Stress Curves in Metallic Alloys, Recrystallization, Prof. Krzysztof Sztwiertnia (Ed.), ISBN: 978-953-51-0122-2, InTech, Available from: http://www.intechopen.com/books/recrystallization/mathematical-modeling-of-single-peak-dynamic-recrystallization-flow-stress-curves-in-metallic-alloys

INTECH
open science | open minds

InTech Europe
University Campus STeP Ri
Slavka Krautzeka 83/A
51000 Rijeka, Croatia
Phone: +385 (51) 770 447
Fax: +385 (51) 686 166
www.intechopen.com

InTech China
Unit 405, Office Block, Hotel Equatorial Shanghai
No.65, Yan An Road (West), Shanghai, 200040, China
中国上海市延安西路65号上海国际贵都大饭店办公楼405单元
Phone: +86-21-62489820
Fax: +86-21-62489821

IntechOpen